



Inside the Lévy Dragon

Author(s): Scott Bailey, Theodore Kim, Robert S. Strichartz

Source: *The American Mathematical Monthly*, Vol. 109, No. 8 (Oct., 2002), pp. 689-703

Published by: Mathematical Association of America

Stable URL: <http://www.jstor.org/stable/3072395>

Accessed: 25/03/2009 14:33

Your use of the JSTOR archive indicates your acceptance of JSTOR's Terms and Conditions of Use, available at <http://www.jstor.org/page/info/about/policies/terms.jsp>. JSTOR's Terms and Conditions of Use provides, in part, that unless you have obtained prior permission, you may not download an entire issue of a journal or multiple copies of articles, and you may use content in the JSTOR archive only for your personal, non-commercial use.

Please contact the publisher regarding any further use of this work. Publisher contact information may be obtained at <http://www.jstor.org/action/showPublisher?publisherCode=maa>.

Each copy of any part of a JSTOR transmission must contain the same copyright notice that appears on the screen or printed page of such transmission.

JSTOR is a not-for-profit organization founded in 1995 to build trusted digital archives for scholarship. We work with the scholarly community to preserve their work and the materials they rely upon, and to build a common research platform that promotes the discovery and use of these resources. For more information about JSTOR, please contact support@jstor.org.



Mathematical Association of America is collaborating with JSTOR to digitize, preserve and extend access to *The American Mathematical Monthly*.

<http://www.jstor.org>

Inside the Lévy Dragon

Scott Bailey, Theodore Kim, and Robert S. Strichartz

1. INTRODUCTION. The famous dragon of Paul Lévy, shown in Figure 1, first appeared in print in 1938 [4]. An English translation of Lévy's article, along with his original handdrawn diagrams and more recent computer images, may be found in [3]. Lévy studies the dragon in the context of general families of self-similar curves in the plane, generalizing the von Koch curve. He singles it out for special attention because of its remarkable tiling property, which will play an important role in our discussion. On the other hand, we will treat the dragon as a subset of the plane, and will not make use of the fact that it can be generated as a curve.

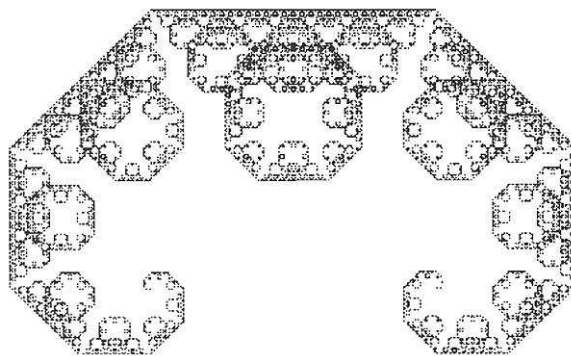


Figure 1. The Lévy dragon.

Images like Figure 1 have appeared in many books and papers, so it is fair to say that the Lévy dragon is one of the standard examples from the world of fractals. (In more technical terms, the Lévy dragon is the invariant set for a linear iterated function system satisfying the open set condition.) It has a more complicated structure than the von Koch curve or the Sierpinski gaskets and carpets, but it is a lot simpler than the Julia sets and Mandelbrot set in complex dynamics. Although a lot is known about the Lévy dragon, we will show that the simple question “What does this dragon really look like?” has not previously received an adequate response.

Lévy proved that his dragon is a tile; in particular, it has an interior (Baire Category Theorem). Neither of these statements is apparent from the picture. The picture does suggest correctly that the dragon is connected, but the interior is disconnected. The interior turns out to be made up of a countable number of components. The largest of these components is quite small, a mere speck on the scale of Figure 1. Thus it is safe to say that Figure 1 is more an image of the boundary of the dragon than of the full dragon itself. The boundary of the dragon is a fractal of dimension $1.934007182988290978 \dots$. This value was computed by two entirely different methods in [2] and [5]. One might then expect that the components of the interior of the dragon have fractal boundaries. They do not. The largest component is a hexagon. Some of the components are finite polygons, and some are infinite polygons, but all have one-dimensional boundaries of finite length. One might expect that the components would come in many (perhaps infinitely many) shapes. This does not appear to

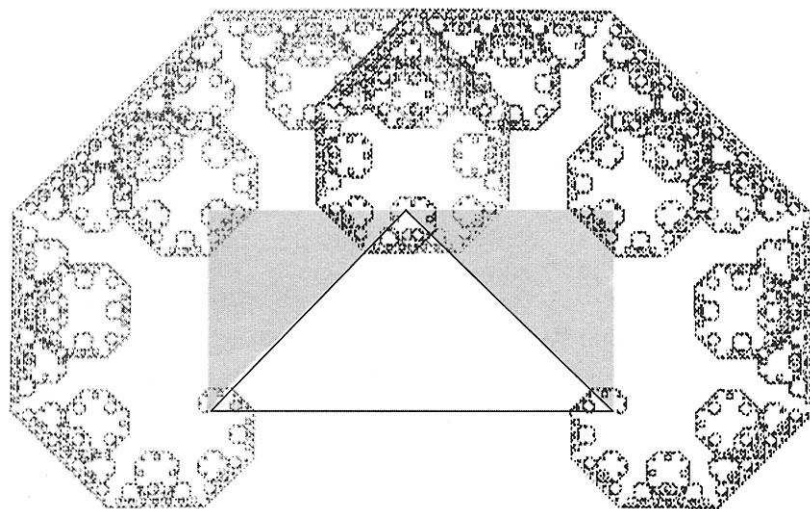


Figure 2. Two dragons combine to make one larger dragon, illustrating identity (1). Also shown are a large triangle (edges drawn) and two smaller triangles (lightly shaded). The large triangle is denoted T in (2) and (3), and the smaller triangles are F_1T and F_2T . Note that only a small portion of the dragon lies inside T .

be the case. We have identified only sixteen different shapes, and it seems unlikely that there are more.

The components of the dragon are completely tame. However, there are still aspects of the dragon that are not tame, relating to the way the components fit together. The dragon is a self-similar set, and Figure 2 shows how it is made up of two similar copies of itself, contracted by a factor of $1/\sqrt{2}$ and rotated through the angle $\pi/4$ clockwise and counterclockwise, respectively. This figure also displays one large and two small triangles. If F_1 and F_2 denote the similarity transformations that map the large triangle onto each of the small ones, keeping the lower common vertex fixed, then the identity

$$D = F_1D \cup F_2D \quad (1)$$

uniquely characterizes the dragon D among nonempty compact subsets of the plane. Since $2(1/\sqrt{2})^2 = 1$, the interiors of F_1D and F_2D must be disjoint, but it is clear from Figure 2 that there are regions where F_1D and F_2D intersect. Components of the interior D^0 of D lying in such regions are made up of unions of components of F_1D^0 and F_2D^0 . We will see that it takes infinitely many components of F_1D^0 and F_2D^0 to create a single component of D^0 , and that these components are combined in quite complicated and intriguing ways. (*Parental advisory:* This paper contains explicit scenes of what might be described as dragons mating.)

The dragon can also be thought of as consisting of a “central hump” and a countable number of smaller humps (similar copies of the central hump). These humps intersect at single points, so components of the interior are entirely contained in a single hump. We leave it as an exercise for the reader to show that the central hump is itself a self-similar set made up of nine copies of itself, satisfying an identity analogous to (1) with nine mappings of varying contraction ratios.

2. HOW TO FAKE A DRAGON. According to the general theory of self-similar fractals [1], [4], the identity (1) tells us how to create approximations to the dragon D : start anywhere, and iterate. Although we *may* start anywhere, it is usually better to

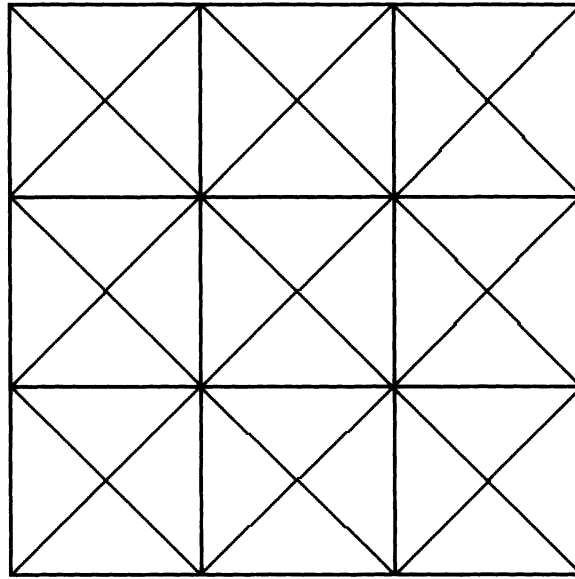


Figure 3. A portion of the tiling of the plane by triangles congruent to T .

make a careful choice of initial set, and so we choose T , the large triangle in Figure 2. The reason for this choice is that under the action of a certain group G of Euclidean isometries T tiles the plane; i.e.,

$$\mathbb{R}^2 = \bigcup_{g \in G} gT \quad (2)$$

and the interiors of the triangles gT are pairwise disjoint (see Figure 3), and we will eventually see that D does so as well.

To describe the iteration process, we let $w = (w_1, w_2, \dots, w_m)$ denote a word of length $|w| = m$, each w_j chosen from $\{1, 2\}$, and write $F_w = F_{w_1} \circ F_{w_2} \circ \dots \circ F_{w_m}$. Define

$$D_m = \bigcup_{|w|=m} F_w T. \quad (3)$$

The level m approximate dragon D_m is the union of 2^m nonoverlapping triangles whose scale is reduced by the factor $2^{-m/2}$ from that of T . Thus the area of each triangle of D_m is reduced by a factor of 2^{-m} , meaning that the total area of D_m is the same as the area of T . In fact, it is a simple exercise to see that each D_m tiles the plane under the action of G , meaning again that

$$\mathbb{R}^2 = \bigcup_{g \in G} gD_m \quad (4)$$

and that the sets gD_m have pairwise disjoint interiors. It is difficult to depict this tiling in black and white, but there is a color plate in [3] that does this. In Figure 4 we display D_m for $1 \leq m \leq 8$ to illustrate that D_m converges to D , but we stress that the convergence is slow. The algorithm for computing D_m inductively is extremely simple: we just replace every triangle T' in D_{m-1} by the pair of smaller triangles related to T'

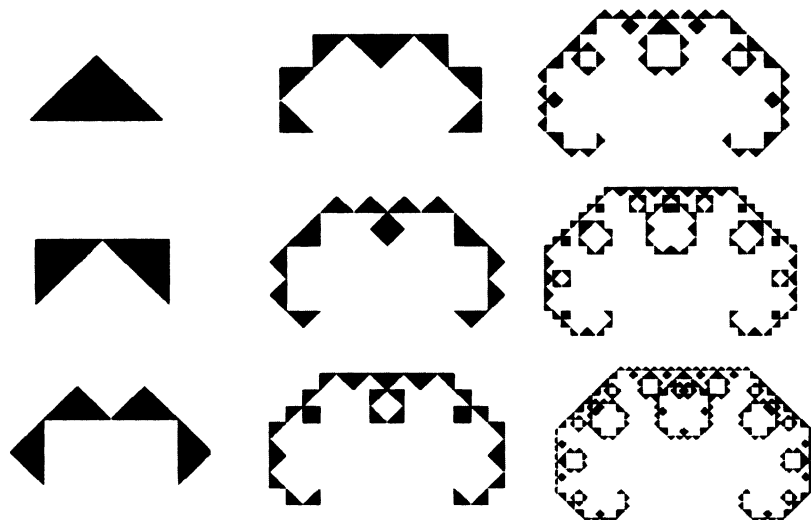


Figure 4. The triangle T and the first eight approximate dragons D_m generated by replacing each triangle T' in D_{m-1} by two similar triangles touching T' along the short sides of T' .

as shown in Figure 2. The thing to keep in mind is that, if you replace each triangle $F_w T$ in D_m with the corresponding reduced dragon $F_w D$, you will get D exactly (this follows from (1) by iteration). Since T and D are quite dissimilar, there will be a considerable discrepancy between D_m and D in details on the length-scale of $2^{-m/2}$. It is only when you look on a larger scale that you can accept the “fake” dragon D_m as a good substitute for the real dragon D . Nevertheless, one can obtain a good deal of information about the real dragon from the fakes.

In particular, we want to focus on a very important question. Let \mathcal{J}_m denote the collection of all triangles in the tiling of the plane by the individual triangles $gF_w T$ of D_m and its G -images. (N.B. The isometry group associated with the tiling by the members of \mathcal{J}_m is larger than G .) Each triangle in \mathcal{J}_m has sides reduced by $2^{-m/2}$ compared with the triangles in (2), and when m is odd the tiling \mathcal{J}_m is rotated by $\pi/4$ compared with the tiling (2).

Question 1. Given a fixed triangle T' in \mathcal{J}_m , when is it entirely contained in D ?

Answer. This happens if and only if all fifteen triangles in \mathcal{J}_m that intersect T' (including T' itself) are in D_m . (We will say T' passes or fails the 15-test for D_m .)

Figure 5 shows the configuration of fifteen triangles in \mathcal{J}_m that intersect T' (the shaded triangle). Label these triangles T'_1, \dots, T'_{15} , and let D'_1, \dots, D'_{15} denote the corresponding dragons ($D'_j = F_w D$ if $T'_j = F_w T$) at level m (no relation to D_m), part of the tiling of \mathbb{R}^2 by dragons of this size. By looking at Figure 5 you should be able to convince yourself of the following two facts:

- Fact 1:* No other dragon of level m intersects the interior of T (a few intersect the boundary of T alone).
- Fact 2:* All fifteen dragons D'_j intersect the interior of T' (to see this you will have to imagine the triangles replaced by the corresponding dragons).

With the aid of these two facts it is easy to verify the answer given for Question 1, since they imply that the interior of T' is contained in $\bigcup_{j=1}^{15} D'_j$ and not in any union

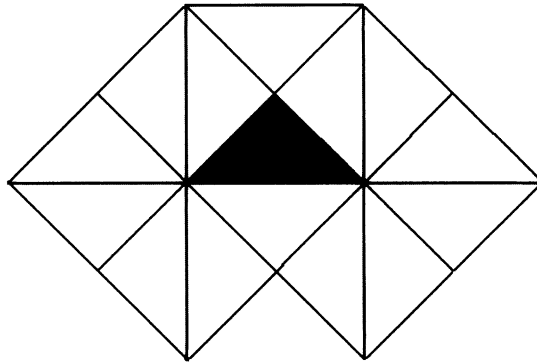


Figure 5. The configuration of fifteen triangles from \mathcal{J}_m that touch the shaded triangle (the shaded triangle is counted as one of the fifteen). These are exactly the triangles from \mathcal{J}_m whose corresponding dragons intersect the interior of the shaded triangle.

of fewer than these fifteen dragons. So

$$\text{int}(T') \subseteq \bigcup_{j=1}^{15} D'_j \subseteq D$$

if all fifteen triangles are in D_m . Since D is closed, we see also that T is contained in D . Conversely, if one of the fifteen triangles is not in D_m , then the interior of the corresponding dragon D'_j is disjoint from D , so a portion of T is not in D .

We can use the answer to Question 1 to devise a simple algorithm for generating a sequence of sets I_m that approximate the interior of the dragon from within. We simply take I_m to be the interior of the union of all triangles in \mathcal{J}_m that pass the 15-test for D_m . Because the \mathcal{J}_m -tilings are nested, the sequence of interior approximations is increasing. Note that I_m is empty for a while (until $m = 14$). The algorithm for computing both D_m and I_m is approximately local, so if we want to explore the portion of the interior in some small region we only have to keep track of triangles in a neighborhood of that region. This is fortunate because we need to go to large values of m (around 35, say) in order to exploit this feature and there are 2^m triangles in D_m .

Figure 6 shows the sequence $I_m \cap R$ for R a fixed rectangle and $m = 14, 15, 16$, and 17. We have chosen R to be a neighborhood of the first triangles that appear in I_{14} (actually there are two symmetric components of I_{14} , of which we have chosen one). Notice that as m increases the components of I_m grow in size, new components emerge, but we never see two components merge together. This is true not just for the region shown, but for all regions we have observed.

Conjecture 1. Distinct components of I_m are contained in distinct components of D^0 .

Another striking observation is that some components stop growing altogether after a few steps. The original component of I , for example, grows into a hexagon in two steps, and then stops growing. In fact, we can show that this hexagon is a component of the interior of D . To do this we need to show that each side of the hexagon belongs to the boundary of D .

Question 2. Given a line segment L (or a more general set L) in D , how can we tell (from D_m alone) if L lies in the boundary of D ?

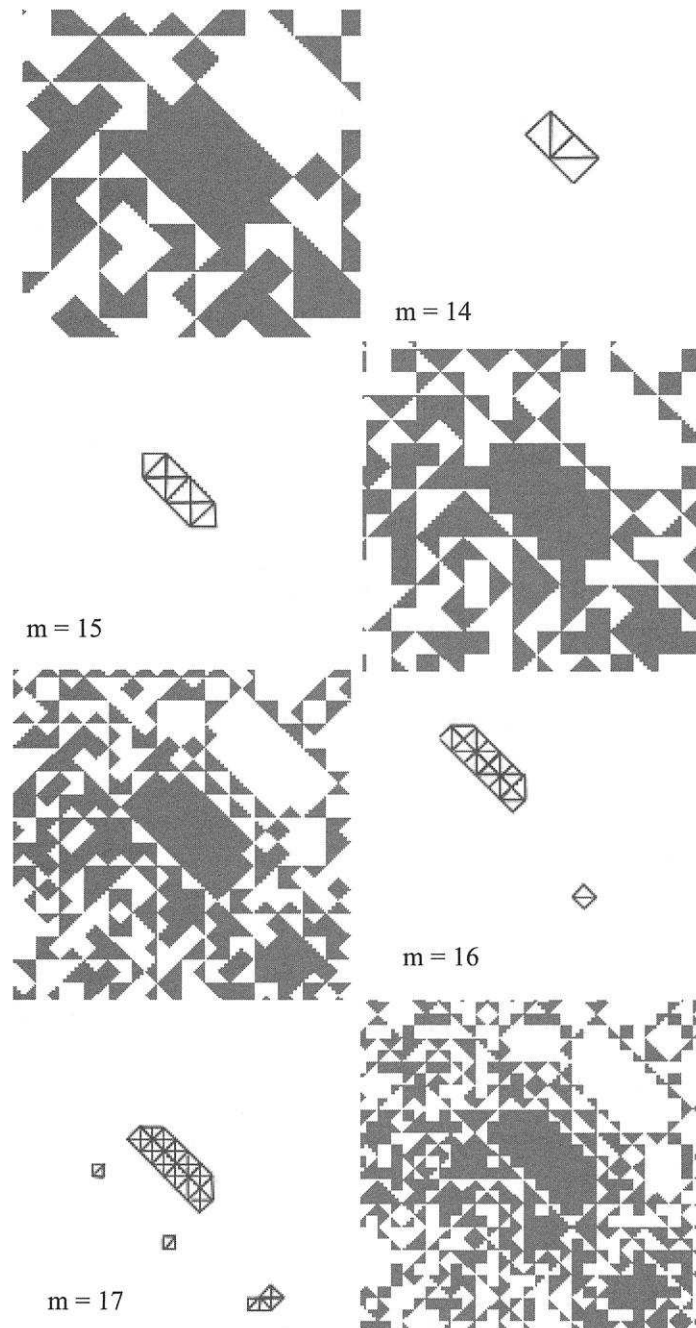


Figure 6. A zoom of a fixed region in D_m and I_m for $m = 14, 15, 16$, and 17 . Observe that the original component in I_{14} grows until it becomes a hexagon in I_{16} , but then stops growing. New components enter in I_{16} and I_{17} , but are disjoint from earlier components.

Answer. This will be the case if L is contained in a dragon at level m whose corresponding triangle in \mathcal{J}_m is not contained in D_m .

The reason is simply that, for each triangle T' in \mathcal{J}_m , the level m dragon corresponding to T' must belong to one of the dragons in the tiling $\cup gD$; if it does not belong to D , it can only intersect D on the boundary. Note that the condition is not necessary, for there may be more than one dragon of level m containing L .

It is especially easy to use the answer to Question 2 when L is the interior of a side of one of the triangles in I_m . We discover an all-or-nothing criterion: either L lies entirely in the boundary of a component of D^0 , or it lies in the interior of a component of D^0 (and this becomes apparent in I_{m+1}).

Border algorithm. Let T' be a triangle from \mathcal{J}_m that appears for the first time in I_m (so T' is not contained in I_{m-1}). For each side S_j of T' there is a control triangle T'_j in \mathcal{J}_m (as shown in Figure 7) such that

- (i) if T'_j is not in D_m , then S_j belongs to the boundary of the component of D^0 containing T' ;
- (ii) if T'_j is in D_m , then the interior of S_j (i.e., S_j less its endpoints) belongs to the component of D^0 containing T' .

It is easy to implement (i) to draw solid borderlines along sides of triangles in I_m that will be part of the boundaries of the developing components. Note that (ii) implies that all nonbordered sides will see growth in I_{m+1} . Moreover, (i) and (ii) imply that any component of I_m that does not grow in I_{m+1} is already a complete component of D^0 .

To verify part (i) of the border algorithm we only need to look at Figure 7 and observe that the level m dragon associated with T'_j contains the side S_j . To verify part (ii) we need separate arguments for the long side S_3 and for the short sides S_1 and S_2 . Since T' lies in I_m , it passes the 15-test for D_m . Consider the triangle T'_3 in \mathcal{J}_m obtained from T' by reflecting it across the long side S_3 . Applying the 15-test to T'_3 , we see that fourteen of the fifteen required triangles are in D_m (because of the 15-test for T'), and the remaining one is exactly T'_3 . So T'_3 is contained in D_m , which makes T'_3 a subset of I_m and places S_3 in the interior of D . Of course this just means that we have to look at a whole component of I_m : all the long sides in the interior of the component of I_m are obviously in the interior of D^0 , and all the remaining long sides

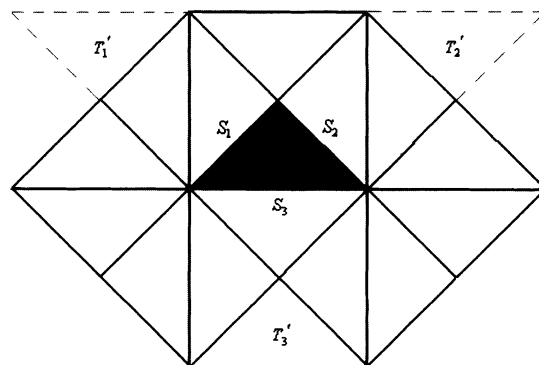


Figure 7. The same configuration of fifteen triangles shown in Figure 5, with the three control triangles T'_j that determine whether or not the interior of the side S_j of the shaded triangle belongs to the interior or boundary of D (and the component of D^0 containing the shaded triangle).

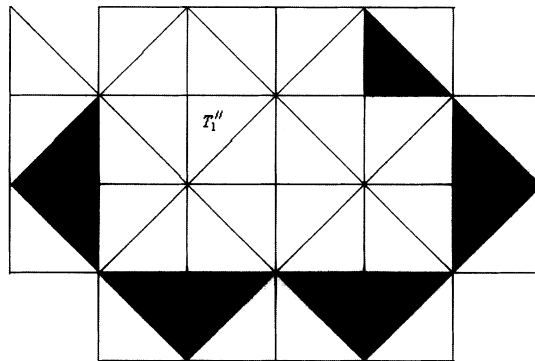


Figure 8. The thirty-two \mathcal{J}_{m+1} -triangles generated by the sixteen \mathcal{J}_m -triangles consisting of T_1' and the fifteen triangles of Figure 5 (the black triangles are not included among the thirty-two triangles). The triangle labeled T_1'' has S_1 as a side, and passes the 15-test for D_{m+1} , thus placing the interior of S_1 in the interior of D .

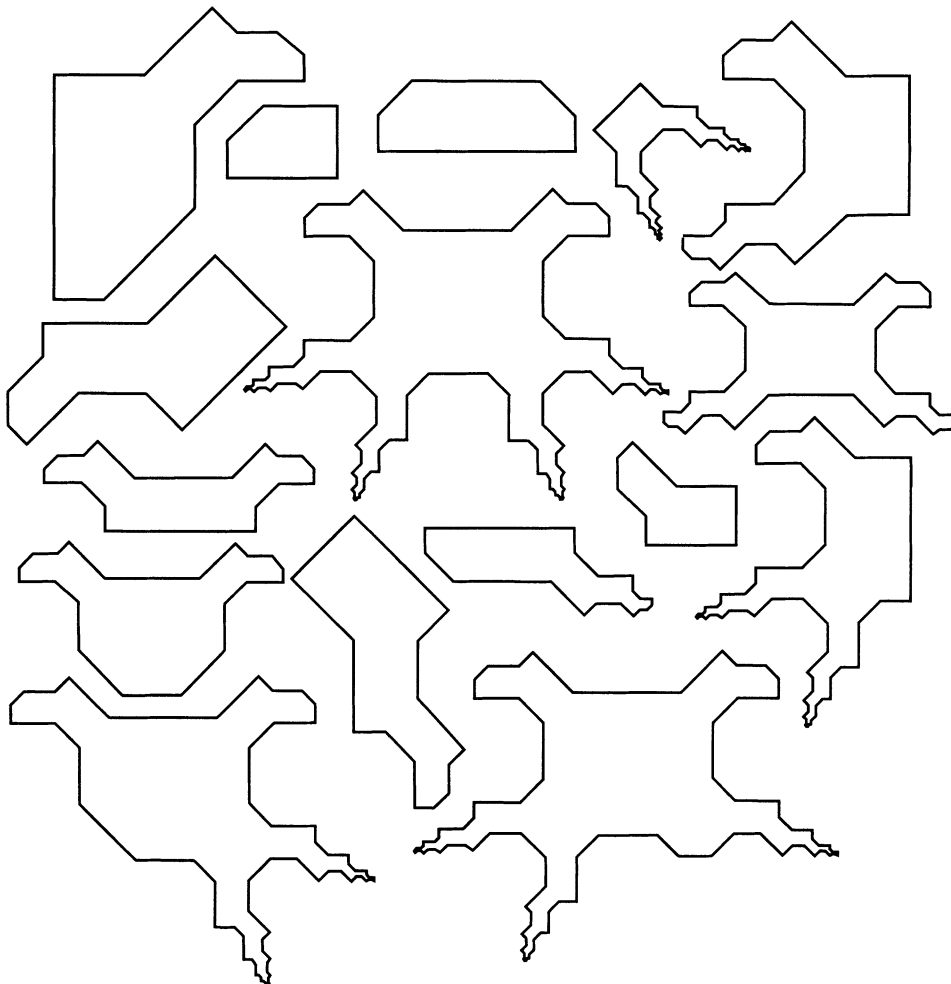


Figure 9. Sixteen shapes of components of the interior.

are part of the boundary. Another way of saying this is that all growth from I_m to I_{m+1} occurs along short edges of triangles in \mathcal{J}_m .

To verify part (ii) for a short edge, say S_1 , requires that we pass to the next level. Let T_1'' denote the triangle from \mathcal{J}_{m+1} lying across the edge S_1 from T' (then S_1 becomes the long side of T_1''). Starting from the sixteen triangles from \mathcal{J}_m that we know are in D_m (the fifteen from the 15-test for T' and the control triangle T_1'), we obtain thirty-two \mathcal{J}_{m+1} -triangles in D_{m+1} , as shown in Figure 8. It is clear from this figure that T_1'' passes the 15-test for D_{m+1} ; hence T_1'' lies in I_{m+1} , putting S_1 in the interior of D^0 .

3. COMPONENTS OF THE INTERIOR. By running the algorithms to generate D_m and I_m , using the border algorithm to mark off boundary edges of components of I_m , and zooming in on regions of interest, we were able to discover sixteen different shapes of components of the interior. These are shown in Figure 9. The programs we used are available on the web site <http://www.mathlab.cornell.edu/~twk6/>. The reader is invited to look for these shapes and more—if there are any more. (Note that we count the mirror image of a shape as the same shape.)

Conjecture 2. Every component of the interior is similar to one of the sixteen shapes shown in Figure 9.

There are two types of shapes: ordinary polygons, and polygons with infinitely many sides (but with a boundary of finite length). In fact the infinite-sided polygons may be described in terms of “legs.” The basic structure of a leg is shown in Figure 10. In passing from I_m to I_{m+1} , the leg adds four triangles from \mathcal{J}_{m+1} , three of which are adjacent and add on to the bottom of the leg, and one of which adds a corner to a \mathcal{J}_m -triangle added in the previous step. Note that the two boundary curves of the leg are self-similar piecewise linear curves, and they are similar to each other. A component shape may have up to four legs. A four-legged shape, called the “baby dragon,” is generated anytime D_m contains a set of fourteen triangles in the configuration shown in Figure 11, where the two shaded triangles are not part of D_m . (The baby dragon is the only four-legged shape in Figure 9, and it is also featured later in Figure 15.)

The baby dragon shape is clearly visible in Figure 1 as a component of the complement of D , and many leg shapes appear in parts of the unbounded component of the complement of D . In fact, the identical shapes appear as components of D^0 and as bounded components of the complement of D . The reason for this is that the configuration in Figure 11 appears in D_m for large enough m . Denote the two shaded triangles by T' and T'' , and their corresponding dragons by D' and D'' . Now $D' \cup D''$ is in the complement of D and contains the central hump H of a dragon, but the boundary of H is in D . Thus every bounded component of the complement of H is a component of D^0 . Since every bounded component of the complement of D is similar to a bounded component of the complement of H , we have established the correspondence in one direction: bounded components of the complement of D are similar to components of D^0 . But the reverse direction is essentially the same: a component of D^0 is similar to a component of the interior of any hump, and in particular of the hump H .

In short, the shapes that make up the interior of D are not really “new” shapes: they have been visible all along in the pictures of D as components of the complement. There is reason to believe that the baby dragon is the essential shape.

Conjecture 3. Every component of D^0 is obtained from a baby dragon by cutting along a finite number of line segments (this is the same thing as intersecting the baby dragon with a finite number of half-planes).

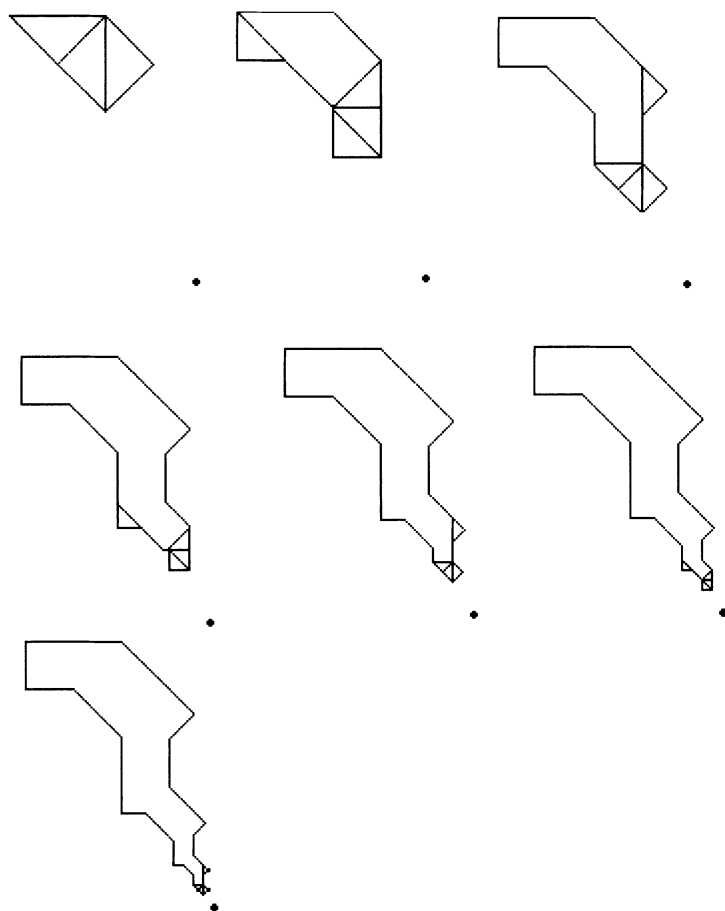


Figure 10. Seven steps of the construction of a leg, as seen in I_m, \dots, I_{m+6} (the dot represents the tip of the leg).

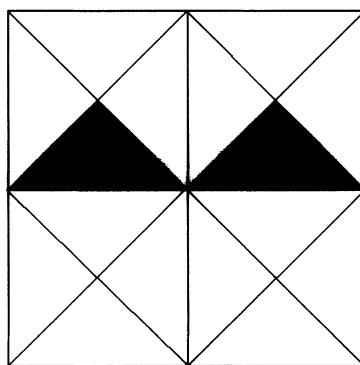


Figure 11. The configuration of fourteen triangles in D_m and two shaded triangles not in D_m that gives rise to a baby dragon.

We now give a proof that the boundary of every component of D^0 is tame. This would be an immediate consequence of Conjecture 2 or 3.

Theorem. *Every component of D^0 has a boundary of finite length made up of a finite or countable number of line segments.*

Proof. Observe that the central hump has outer boundary (the boundary of the unbounded component of its complement) made up of a countable number of line segments of finite total length (the lengths form a geometric progression with ratio $1/\sqrt{2}$). The same is then true of the dragon itself, since the sequences of humps are scaled by a factor of $1/\sqrt{2}$.

Consider a component U of D^0 , and let m mark the time a triangle T of I_m contained in U first appears. Let \mathcal{J}'_m denote the set of \mathcal{J}_m -triangles not in D_m with the following property: if D' is the dragon associated with T' in \mathcal{J}'_m , then D' intersects U . There are only a finite number of triangles in \mathcal{J}'_m . Furthermore, T and all triangles touching it are not in \mathcal{J}'_m . Thus U is a component of the complement of the union of the D' dragons (associated to the \mathcal{J}'_m -triangles). Because U is connected it is disjoint from the bounded components of the complements of D' dragons. Thus the boundary of U is a subset of the union of the outer boundaries of a finite number of dragons. ■

4. GEOMETRY OF INTERIOR COMPONENTS. The boundary of a component of D^0 is a finite or infinite polygonal line, so the interesting points on the boundary are the *corners* where two line segments meet. The corners are either convex or concave (viewed from the inside). In principle there should be six possible arrangements, since the line segments arise from \mathcal{J}_m -triangles: convex or concave angles of $\pi/4$, $\pi/2$, and $3\pi/4$. But as a matter of fact we observe only three.

Conjecture 4. Corners are either convex with angles $\pi/2$ or $3\pi/4$, or concave with angle $3\pi/4$.

In particular, the absence of a convex corner of angle $\pi/4$ means that if T' is a \mathcal{J}_m -triangle in I_m —so T' passes the 15-test for D_m —then D_m must also contain either the control triangle T'_3 or both control triangles T'_1 and T'_2 . Because the control triangles are so widely separated, it is hard to conceive of an argument that would explain this relationship. The absence of both T'_1 and T'_2 is allowed, since it produces a convex corner with angle $\pi/2$, something that is observed.

The absence of concave corners with angle $\pi/2$ or $\pi/4$ is easy to explain. One way for the $\pi/2$ angle to occur would be to have three triangles from \mathcal{J}_m meeting at their right angle vertex belong to I_m , while the fourth member of \mathcal{J}_m with a right angle at that vertex is not in I_m . But the fact that the first three triangles pass the 15-test implies that the fourth triangle also passes it, for any \mathcal{J}_m -triangle that touches the fourth must also touch one of the other three. The other possibility is that six \mathcal{J}_m -triangles sharing a vertex at which each has angle $\pi/4$ be in I_m . This forces the other two members of \mathcal{J}_m meeting at the same point to be in I_m . The same argument rules out convex corners of angle $\pi/4$.

Another interesting geometric question concerns the way two components of D^0 may abut (meaning that their boundaries have a common point). Note that the connectivity of D does not imply that any components of D^0 touch in this sense. It only implies that there must exist components of D^0 arbitrarily close to any given component. Indeed, we believe that there are isolated components of D^0 (components that do not touch any other component), namely, components with either of the two convex

polygon shapes (recall Figure 9). In fact, we observe only one type of touching: the tip of a leg touching a corner.

Conjecture 5. Two components of D^0 can touch only if a corner of one component coincides with the tip of a leg of the other. Moreover, every concave corner of a component of D^0 is such a contact point.

It is not difficult to see that points in the interior of a line segment on the boundary of a component of D^0 cannot be touching points with other components: such a segment would arise through alternative (i) of the border algorithm, so the complement of D would contain a dragon lying on the other side of this segment. Thus the segment would be an outer boundary segment of a hump that is in the complement

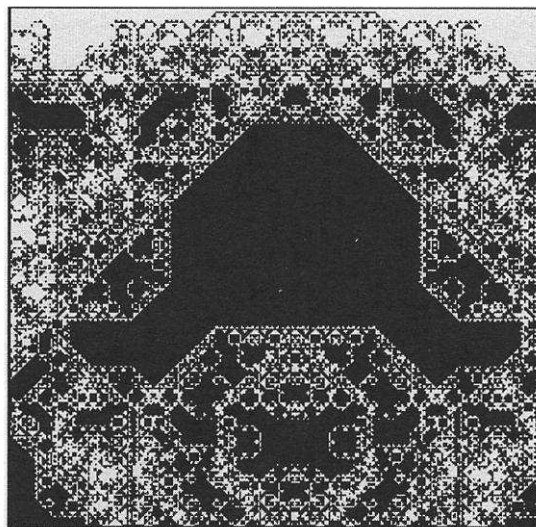


Figure 12. A polygonal component C shown in a zoom of a D_m approximation.

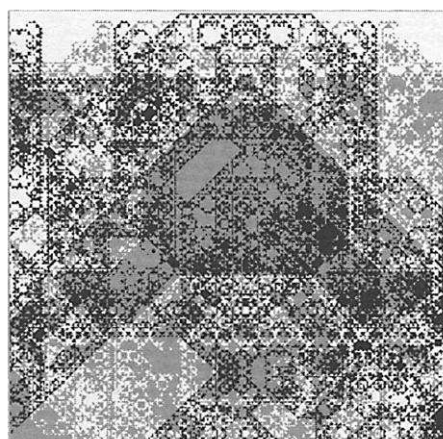


Figure 13. The splitting of Figure 12 into two D_{m-1} approximations in different gray-scales.

of D . From Figure 1 we see that the segment is touched at its endpoints by tips of legs in the complement of the hump, but by no other components. (This “proof by pictures” is valid because the neighborhood of the segment in the hump is self-similar, ensuring that pictures on smaller scales will look the same.)

Thus the only possible touching points are corners and tips of legs. However, there are many plausible touching configurations, such as two convex right angles, that are ruled out by Conjecture 5. Also, it is not clear why every concave corner is touched.

5. DRAGONS MATING. The identity (1) shows how to mate two small dragons to get one larger one. What happens to the components of D^0 in the process? Of course, some components are entirely contained in either F_1D or F_2D , so the question really concerns the components that intersect both of these sets. If C denotes such a component of D^0 , then $C \cap F_1D$ is made up of a union of images F_1C_j of other components C_j of D^0 , together with parts of their boundaries; the same holds true for $C \cap F_2D$. In principle one could build any of the shapes in Figure 9 by assembling a finite number of other shapes, but in the mating of dragons it appears that infinitely many components F_1C_j and F_2C_j are required.

Conjecture 6. Let C be a component of D^0 . If $C \cap F_1D$ and $C \cap F_2D$ are both nonempty, then each of these sets contains infinitely many components of F_jD^0 .

Figures 12–17 show two examples of such decompositions. Many more may be seen on the web site. These were simply obtained by running the algorithm to generate the dragon simultaneously on two adjacent triangles using separate colors (gray-scales in the figures here). These two triangles may be thought of as the two central triangles in D_2 , which generate the regions of overlap of F_1D and F_2D . By combining the two types of triangles we obtain a D_m approximation of the component C . Looking at the two types separately, we see a D_{m-1} approximation of many of the components of F_jD^0 . Figures 14 and 17 show the corresponding I_{m-1} interiors. Figure 12 shows a polygonal component, and Figure 15 shows a baby dragon. It is definitely not the case that similar components have similar decompositions. In fact, in Figure 15 you can see several smaller baby dragons, but in Figure 16 they all have different decompositions. Also note that both shapes have a line of symmetry, but the decompositions do not exhibit this symmetry.



Figure 14. The I_{m-1} interior approximations corresponding to Figure 13.

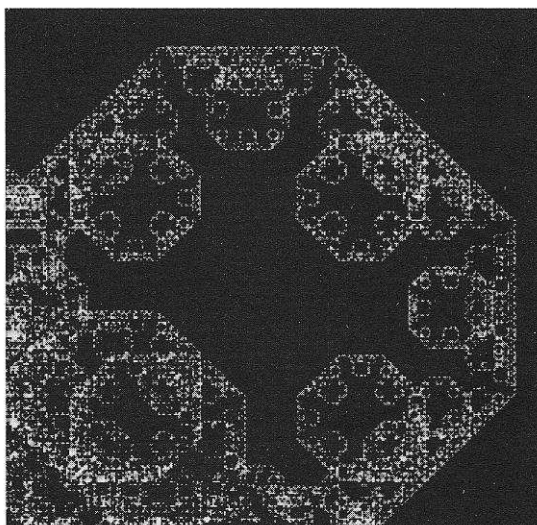


Figure 15. A zoom of a D_m approximation containing a baby dragon (in fact several smaller baby dragons are also visible).

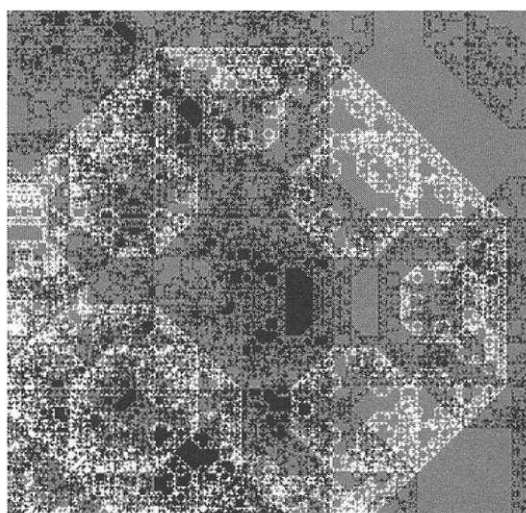


Figure 16. The splitting of Figure 15 into two D_{m-1} approximations in different gray-scales. The decompositions of the different baby dragons are not similar to each other.

It is easy to see that for any shape there are at most a finite number of similarity types of decompositions of components with that shape. Indeed, any such component is produced by the same configuration of triangles in some D_m , and the type of decomposition is determined by how that finite set of triangles is divided up. This gives a rather large (in the millions) upper bound for the number of decomposition types. We have no idea what the actual numbers might be.

ACKNOWLEDGMENT. The research of Strichartz was supported in part by the National Science Foundation, grant DMS-9970337.



Figure 17. The I_{m-1} approximations corresponding to Figure 16.

REFERENCES

1. Michael Barnsley, *Fractals Everywhere*, Academic Press, Boston, 1988.
2. P. Duvall and J. Keesling, The Hausdorff dimension of the boundary of the Lévy dragon, *Int. J. Math. and Math. Sci.* **20** (1997) 627–632.
3. G. A. Edgar, *Classics on Fractals*, Addison-Wesley, Reading, MA, 1993.
4. Kenneth Falconer, *Fractal Geometry: Mathematical Foundations and Applications*, John Wiley & Sons, New York, 1990.
5. P. Lévy, Les courbes planes ou gauches et les surfaces composée de parties semblables au tout, *J. d'Ecole Polytechnique* (1938) 227–247, 249–291.
6. R. Strichartz and Y. Wang, Geometry of self-affine tiles I, *Indiana Univ. Math. J.* **48** (1999) 1–24.

SCOTT BAILEY is a graduate student in mathematics at Northwestern University. He received his B.A. in mathematics from Cornell University in May 2002. In addition to his work on the Lévy Dragon fractal, he has done research in a variety of fields that include group actions on graphs and homology theory at Louisiana State University with Robert Perlis and Jerome Hoffman, as well as random walks on hyperplane arrangements with Kenneth Brown at Cornell University.

Mathematics Department, Northwestern University, Evanston, IL 60208
smb43@cornell.edu

THEODORE KIM received his bachelor's degree at Cornell University in computer science and is currently working towards a Ph.D. in computer science at the University of North Carolina at Chapel Hill, concentrating in computer graphics. His current research interests include quaternionic Julia set visualization and physically based modeling.

Computer Science Department, University of North Carolina, Chapel Hill, NC 27599
kim@cs.unc.edu

ROBERT S. STRICHARTZ is Professor of Mathematics at Cornell University. Educated at Bronx High School of Science, Dartmouth College, and Princeton University, where he received his Ph.D. in 1966, he was a NATO Postdoctoral Fellow and C.L.E. Moore Instructor at M.I.T. before coming to Cornell in 1969. His research interests include harmonic analysis, partial differential equations, geometric analysis, and fractals. He is the author of the textbook *The Way of Analysis*. He serves as an Executive Editor for *Journal of Fourier Analysis and Applications*, and he directs a summer REU program at Cornell. He received a Lester R. Ford Award for the MONTHLY article "Radon Inversion—Variations on a Theme." His most recent MONTHLY article was "Evaluating Integrals Using Self-similarity."

Mathematics Department, Malott Hall, Cornell University, Ithaca, NY 14853
str@math.cornell.edu